Collective excitations and viscosity in liquid Bi

Matti Ropo, Jaakko Akola, and R. O. Jones

Citation: The Journal of Chemical Physics **145**, 184502 (2016); doi: 10.1063/1.4965429
View online: http://dx.doi.org/10.1063/1.4965429
View Table of Contents: http://scitation.aip.org/content/aip/journal/jcp/145/18?ver=pdfcov
Published by the AIP Publishing

Collective excitations and viscosity in liquid Bi

Matti Ropo,[1,2] Jaakko Akola,[1,2] and R. O. Jones[3,a)]
[1]*Department of Physics, Tampere University of Technology, P.O. Box 692, FI-33101 Tampere, Finland*
[2]*COMP Centre of Excellence, Department of Applied Physics, Aalto University, FI-00076 Aalto, Finland*
[3]*Peter-Grünberg-Institut (PGI-1) and JARA/HPC, Forschungszentrum Jülich, D-52425 Jülich, Germany*

(Received 28 June 2016; accepted 6 October 2016; published online 8 November 2016)

The analysis of extensive density functional/molecular dynamics simulations (over 500 atoms, up to 100 ps) of liquid bismuth at four temperatures between 573 K and 1023 K has provided details of the dynamical structure factors, the dispersion of longitudinal and transverse collective modes, and related properties (power spectrum, viscosity, and sound velocity). Agreement with available inelastic x-ray and neutron scattering data and with previous simulations is generally very good. The results show that density functional/molecular dynamics simulations can give dynamical information of good quality without the use of fitting functions, even at long wavelengths. *Published by AIP Publishing.* [http://dx.doi.org/10.1063/1.4965429]

I. INTRODUCTION

Collective modes in liquids have been investigated in recent years using inelastic neutron scattering (INS) and inelastic x-ray scattering (IXS). In addition to longitudinal acoustic (LA) modes (e.g., in liquid alkali metals),[1] there is now clear evidence that transverse acoustic (TA) modes have been identified in a range of elements, including Ga,[2] Sn,[3] Fe and Cu,[4] and Zn.[4,5] The TA modes show up as weak peaks in the dynamic structure factor at energies below those of the LA modes. Parallel to these developments there have been detailed studies of the static, dynamic, and electronic properties of liquids using molecular dynamics (MD) simulations, often with the density functional (DF) theory[6] as the basis of force and energy calculations. These have included studies of Si,[7,8] Ga,[2,9] Mg,[10] Bi,[11,12] Sn,[13] Pb,[14] and Al[15] as well as 58 liquid elements at their triple points (125 atoms in the simulation cell, except for Li, Na, Mg, and Al with 250–384 atoms).[16]

The computational demands presented by DF/MD calculations have led to the use of a number of simplifying assumptions. While the simulations on Pb[14] are impressive in both sample size (13 500 atoms) and time (1.2 ns), the interactions within the system are described by the semi-empirical embedded atom model. A simplification of the standard (Kohn-Sham) DF calculations[6] is provided by "orbital-free" methods, where approximations to the kinetic energy of the non-interacting system are introduced. Simulations with 2000 ions have been performed with this approach in Si (50 ps data collection, 1740 K),[7] Ga (80 ps, three temperatures),[9] and Mg (50 ps, 953 K).[10] Calculations using DF/MD calculations without approximations to the non-interacting kinetic energy have been limited, however, to Sn (64 atoms, 108 ps, three temperatures),[13] Bi (124 atoms, 40 ps, 600 K),[11] and Fe (120 atoms, 40 ps, 1873 K).[17] In addition to having a larger fraction of atoms close to a neighboring cell (larger "finite size effects"), small simulation cells mean that the lowest wave-vector that can be considered ($2\pi/L$ for a cubic cell of side L) is correspondingly larger.

Bismuth is a group 15 (pnictogen) element with unusual properties and is the subject of the present study. Over 80 years ago, Jones[18] explained the high diamagnetism, low (semimetallic) conductivity, and the A7 (rhombohedral) structure as a distortion of a simple cubic structure brought about by the existence of a large (Jones) zone containing five valence electrons per atom. This mechanism, often referred to today as a "Peierls instability,"[19] has been invoked in discussions of the structures of group 15 liquids, all of which are characterized by a short-range order similar to that of the underlying A7 structure.[20]

Over the past 60 years, liquid bismuth has attracted much attention. Bi has excellent neutron scattering properties, and the liquid shows a variety of interesting structural properties, including an unusual pressure-temperature phase diagram.[21] Earlier inelastic neutron scattering (INS) measurements showed clear evidence of collective density fluctuations.[22–24] This work has been summarized in detail by Inui *et al.*,[12] who also described inelastic x-ray scattering (IXS) measurements on liquid Bi with distinct inelastic modes at 573 K with approximately constant dispersion between 0.7 $Å^{-1}$ and 1.5 $Å^{-1}$.[12] Supporting DF/MD simulations (128 atoms, 144 ps) also showed collective modes with almost constant frequency in this range.

We described recently a study of Bi_n clusters and of liquid Bi at 573, 773, 923, and 1023 K using DF/MD simulations of more than 500 atoms up to 100 ps.[25] We discussed, in particular, the temperature dependence of the electronic and geometrical structures, including trends in the nearest neighbor, bond angle, and ring distributions, pair distribution functions $g(r)$, structure factor $S(q)$, and power spectra. We noted structural parallels between the cluster and liquid phases. The analysis is extended here to a detailed study of the intermediate scattering function, the

a)Electronic mail: r.jones@fz-juelich.de

dynamical structure factor, the collective (LA, TA) modes, the viscosity, and the relationships between these quantities. We keep the use of fitting procedures (memory functions, generalized collective modes, etc.) to a minimum. In the case of longitudinal excitations, for example, we have determined the peak positions from the data without fitting the quasielastic peak or side peaks to assumed shapes. In Sec. II we summarize the method of calculation and the basis of the analysis, and we present and discuss the results in Secs. III and IV, respectively.

II. METHODS OF CALCULATION

A. Density functional calculations

The simulations were carried out with the CPMD program[26] in the Born-Oppenheimer MD mode. Periodic boundary conditions were used with a single point (k = 0) in the Brillouin zone, and the electron-ion interaction was based on the scalar-relativistic Troullier-Martins pseudopotentials[27] for the valence electrons of bismuth ($6s^2 6p^3$). We used nonlinear core corrections,[28] the PBEsol approximation[29] for the exchange-correlation energy functional, and a kinetic energy cutoff of 20 Ry for the plane wave basis. Spin-orbit interactions are not included. While these can affect the energetic ordering of conformers of small clusters, the effect on structures and forces is weaker.[25]

The simulations of liquid Bi were performed in cubic simulation boxes of 540 (573 K) and 512 atoms (773, 923, and 1023 K) in a fixed volume (*NVT* ensemble) using experimental densities for each temperature.[30] Simulations with cells of this size are numerically very demanding, but the resulting structural data are more reliable than those obtained with smaller samples. In the case of crystallization of the amorphous phase change material $Ge_2Sb_2Te_5$, for example, simulations using 460 atoms[31] gave qualitatively different but more convincing results than those with 180 atoms.[32] The starting structures were determined from reverse Monte Carlo (RMC) fits to x-ray diffraction data,[33] the time step was 3.025 fs, and the temperature was controlled by a Nosé-Hoover thermostat.[34] The samples were equilibrated at each temperature for 10 ps before data collection, and the simulation times after equilibration were 100 ps (573 and 1023 K) or 30 ps (773 and 923 K). The pressure inside the cell during the *NVT*-simulation was positive at all temperatures, reflecting the tendency of the PBEsol functional to overestimate interatomic separations. More details are given in Ref. 25.

B. Analysis of results

1. Power spectrum and thermodynamics

The output of the DF/MD simulation includes the coordinates r_i and velocities v_i of all atoms i after each time step. In Ref. 25, we used the former to calculate the diffusion constants D at all four temperatures

$$D = \lim_{t\to\infty} \frac{\langle |r_i(t) - r_i(0)|^2 \rangle}{6t} \tag{1}$$

and the latter to determine (20 000 time steps, ~60 ps) the velocity-velocity autocorrelation function C_v at 573 and 1023 K,

$$C_v(t) = \frac{1}{N}\sum_{i=1}^{N} \frac{\langle v_i(0)\cdot v_i(t)\rangle}{\langle v_i(0)\cdot v_i(0)\rangle}. \tag{2}$$

The Fourier transform of C_v is the vibrational density of states or power spectrum.

Our previous calculations of the power spectra at 573 K and 1023 K[25] showed a peak ~8 meV and a pronounced peak at low frequencies, particularly at 1023 K. Since the vibrational density of states of a solid goes to zero for $\omega = 0$, the first peak is often associated with diffusive or gas-like modes. This is the basis of the decomposition of the power spectrum into "gas phase" (g, diffusive, single-particle) and "solid" (s, collective) components, which contribute to the low-frequency and high-frequency regimes, respectively.[35] This decomposition is facilitated by modeling the latter by a hard-sphere fluid, where the fraction f of the hard-sphere component in the whole system measures its "fluidicity." This assumption, however, can lead to significant overestimates in the entropy of liquid metals.[36]

This approach allows quantum statistics to be incorporated into MD simulations. At low frequencies, the system behaves classically and can be described by the value of the density of states at zero frequency $S(0)$ and the effective "hard sphere" fraction f, while at higher frequencies the motion is sufficiently harmonic that harmonic quantum corrections apply.[37] The approach provides a way to approach the goal of obtaining accurate thermodynamic quantities, such as entropy and free energy, from MD simulations of modest length.[37] It has given encouraging results for Lennard-Jones fluids and is the basis of the TwoPT (two phase thermodynamics) program,[35] which we use below.

2. Dynamical structure factor

The density fluctuations in the liquid can be described by the intermediate scattering function

$$F(q,t) = \left\langle Re\big(n(q,t+t_0)n(q,t_0)\big)\right\rangle, \tag{3}$$

where $\langle \ldots \rangle$ denote averages over all reference times t_0, and $n(q,t)$ is a Fourier component of the density,

$$n(q,t) = \frac{1}{\sqrt{N}}\sum_i \exp(iq\cdot r_i). \tag{4}$$

The index i runs over all particles, whose total number is N. The dynamical structure factor $S(q,\omega)$ is the Fourier transform of $F(q,t)$,

$$S(q,\omega) = \frac{1}{2\pi}\int dt F(q,t)\exp(i\omega t). \tag{5}$$

The wave number q is restricted by the periodic boundary conditions to

$$\mathrm{q} = |q| = \frac{2\pi}{L}|(n_1,n_2,n_3)|, \tag{6}$$

where n_1, n_2, and n_3 are integers and L is the size of the cubic simulation cell. For the simulation at 573 K, the lowest

value of q is 0.236 56 Å^{-1}. Calculations of structure factors and related functions involve averages over all equivalent q vectors with q = $|q|$.

In principle, $F(q,t)$ can also be obtained directly from the (van Hove) time-dependent pair distribution function $g(r,t)$, but we have found that taking the Fourier transform of the current densities leads to numerically more stable results. The calculated $S(q,\omega)$ can be smoothed by applying, for example, a Gaussian window function.[38]

3. Current autocorrelation functions

The current autocorrelation function $C(q,t)$[39] can be calculated directly from the Fourier transform of the particle current $J(q,t)$, which has a longitudinal component

$$J_L(q,t) = \frac{1}{\sqrt{N}} \sum_i q \cdot v_i \exp(iq \cdot r_i) \tag{7}$$

and a transverse component

$$J_T(q,t) = \frac{1}{\sqrt{N}} \sum_i q \times v_i \exp(iq \cdot r_i). \tag{8}$$

The longitudinal component of the current autocorrelation function is

$$C_L(q,t) = \left\langle Re\big(J_L(q,t+t_0)J_L(q,t_0)\big)\right\rangle \tag{9}$$

with a transverse component

$$C_T(q,t) = \frac{1}{2}\left\langle Re\big(J_T(q,t+t_0)J_T(q,t_0)\big)\right\rangle. \tag{10}$$

The factor 1/2 in $C_T(q,t)$ reflects the fact that there are two independent vectors perpendicular to q.

The longitudinal and transverse components of $C(q,t)$ are well-defined and can be evaluated, but we note that the separation into L and T modes in a disordered system is exact only in the limit of long wavelengths. The transverse current can then contribute to the measured (longitudinal) correlation function, as noted by Gaskell and Miller in a study of liquid sodium.[40]

4. Viscosity

A variety of experimental probes, including x-rays and neutrons, couple to longitudinal density fluctuations, but provide no direct information about transverse fluctuations. The shear viscosity η is a rare transport property that couples to the transverse momentum, and this makes viscosity studies particularly valuable. The shear viscosity can be calculated from the transverse current autocorrelation function,[41,42] and its q-dependence can be written as[15,43]

$$\eta(q, z=0) = \frac{n}{q^2} \frac{k_B T/m}{\Psi_T(q, z=0)}, \tag{11}$$

where k_B, T, n, and m are the Boltzmann constant, temperature, and atomic number density and mass, respectively. $\Psi_T(q,z)$ is the Laplace transformation of $C_T(q,t)$, and $\Psi_T(q,z=0)$ is obtained by integrating the normalized transverse-current correlation function.

Extrapolation to $q = 0$ is carried out using an equation suggested by Alley and Alder based on a hydrodynamic model,[44]

$$\eta(q) = \frac{\eta}{1 + a^2 q^2}, \tag{12}$$

where η is the shear viscosity and a is an adjustable parameter.

A simple connection between viscosity η and diffusion constant or diffusivity D is the Stokes-Einstein relationship (SER)[45,46] derived for the diffusion of uncorrelated macroscopic spheres in a liquid

$$D(T)\eta(T) = \frac{k_B T}{c\pi d}, \tag{13}$$

where d is an effective diameter of a sphere, and c is a constant that depends on the boundary conditions between the particle and the fluid (slip: $c = 2$, stick: $c = 3$). The SER is often applied to the diffusion of single atoms or molecules at high temperatures[47] and for predictions if one of these quantities is unknown. Recent studies focused on the reasons for its breakdown in undercooled binary liquids using classical MD[48] and in Al-rich liquid alloys using DF/MD simulations.[49]

III. RESULTS

A. Power spectrum and thermodynamics

Thermodynamic properties of liquid Bi were calculated using the TwoPT program[35] (Sec. II B 1), and the power spectrum and its diffusion (g) and vibration (s) components are shown in Fig. 1. The normalization of the curves is

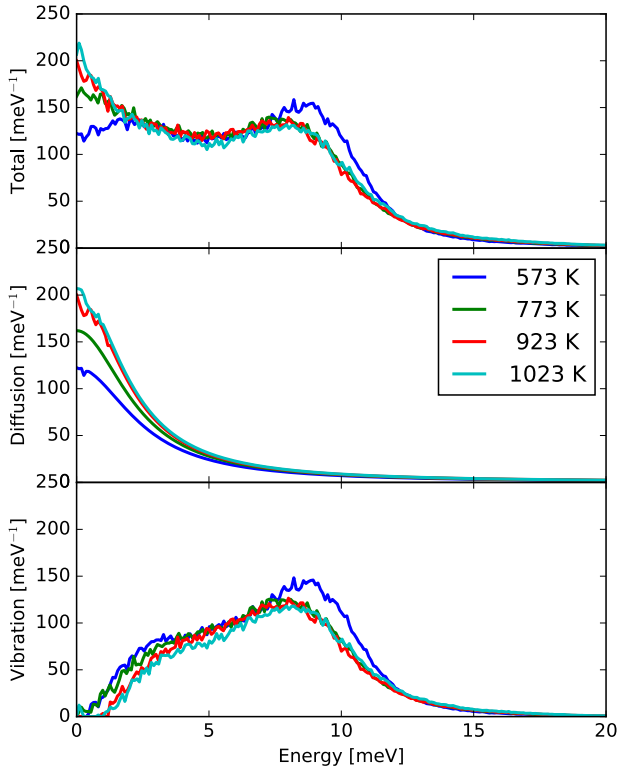

FIG. 1. Power spectra (states per meV) of liquid Bi and its diffusion (g) and vibrational (s) components at four temperatures. The 573 K curve has been renormalized to 512 atoms.

TABLE I. D: diffusion constant (values in brackets from Ref. 25), C_v: heat capacity at constant volume, $S^g(0)$: density of states at $\omega = 0$, S: entropy, ZPE: zero point energy.

T K	D ($10^{-5} \times$ cm^2/s)	C_v (J/mol K)	$S^g(0)$ (cm/mol)	S (J/mol K)	ZPE (kJ/mol)
573	1.88 (1.81)	−0.0366	0.0296	91.3	0.771
773	3.36 (3.28)	−0.0178	0.0392	101.4	0.651
923	4.95 (4.90)	−0.0122	0.0484	106.3	0.627
1023	5.68 (5.47)	−0.0103	0.0501	108.7	0.629

such that the total density of states integrates to the correct number of modes, and the result for 573 K has been scaled to reflect the larger number of atoms (540). The total spectra differ most at low frequencies (<2 meV), where the diffusion term dominates, and these differences are consistent with the different diffusion coefficients (Table I) at different temperatures.

The presence of the low-energy peak in the total power spectrum in Bi at 573 K has been noted previously.[11,25] Its absence at higher temperatures reflects the increasing importance of diffusive (g) modes as the temperature increases. They make up 29% of the total at 573 K, increasing to 42% at 1023 K. At frequencies above 3–4 meV, the vibrational component dominates, showing a distinct peak around 9 meV at 573 K that moves to slightly lower frequencies at higher temperatures. This peak is within the range of frequencies found in crystalline Bi,[50] and its weakening at higher temperatures suggests that aspects of the crystalline structure are still present at 573 K and other temperatures near the melting point.[12,20]

The diffusion coefficient, heat capacity at constant volume, entropy, and zero point energy determined by the TwoPT program[35] are shown in Table I. Of particular interest is the comparison of the diffusion constants D with the values calculated using Eq. (1).[25] The agreement is very good and provides support for the separation of modes used in the TwoPT approach.

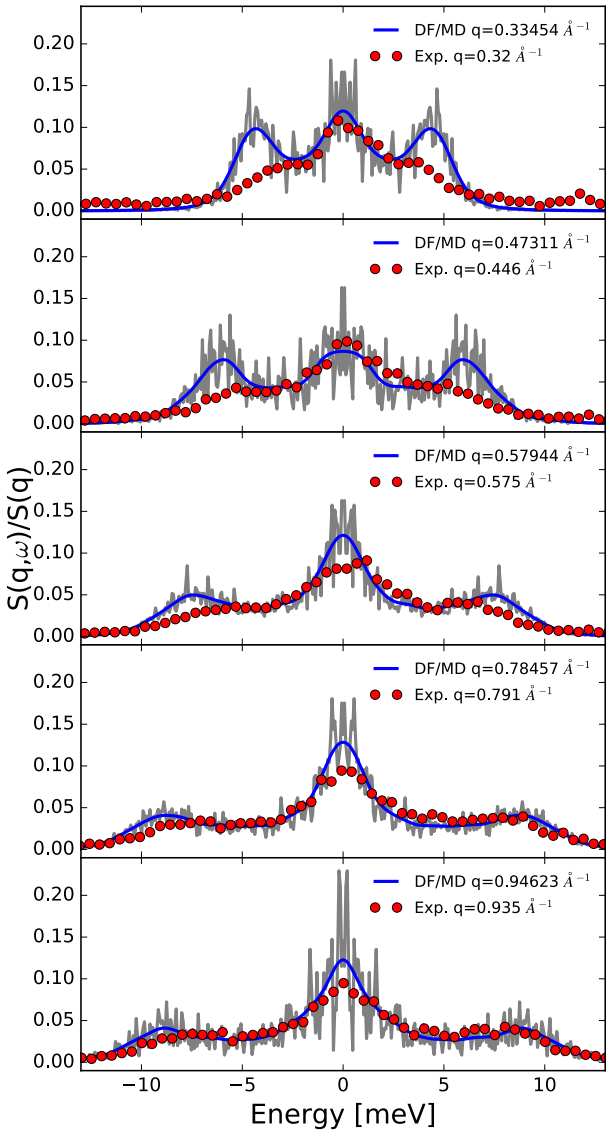

FIG. 2. Ratio of dynamical to static structure factors, $S(q,\omega)/S(q)$, for selected q values at 573 K. Grey: DF/MD results, blue: DF/MD with 3 meV Gaussian broadening, red: experimental IXS (Ref. 12).

B. Dynamical structure factor

The dynamical structure factors $S(q,\omega)$ for selected q values were calculated from the MD trajectories at 573 K and 1023 K using Eq. (5). The ratios to the static structure factors $S(q)$ are compared with experimental IXS results[12,51] in Figs. 2 and 3, respectively. We show results obtained directly from the trajectories as well as those using a Gaussian window function (σ = 3 meV) to reduce numerical noise. Results for additional values of q for both 573 K and 1023 K are provided as the supplementary material. We emphasize again that there are no scaling parameters involved in the comparison of theory and experiment in Figs. 2 and 3.

The overall agreement between theory and experiment is very encouraging. The location of the peak positions in the calculations is correct for small q, but the side peaks are more pronounced than in the experiment (573 K: below 0.5, 1023 K: below 0.4 Å^{-1}). The results at 1023 K (Fig. 3) agree better with experiment for small q values than at 573 K. The DF/MD results for small q are naturally more sensitive to the simulation parameters (cell size, simulation time) than those for larger values of q, for which the peak positions and intensities agree very well.

C. Current correlation functions, collective dynamics

Information about the collective dynamics can be obtained from the longitudinal and transverse current correlation functions (see Sec. II B 3). The 3D-plot of the former [$C_L(q,\omega)$] for 573 K (Fig. 4) shows that the maxima at higher values of q (≥2 Å^{-1}) are accompanied by side peaks and/or shoulders, which makes a definitive assignment of the nature of the collective modes difficult. Selected spectra of the transverse component $C_T(q,\omega)$ at 573 K are shown in Fig. 5, together with the corresponding correlation functions $C_T(q,t)/C_T(q,0)$. It is clear that the correlation function decays more rapidly as q increases.

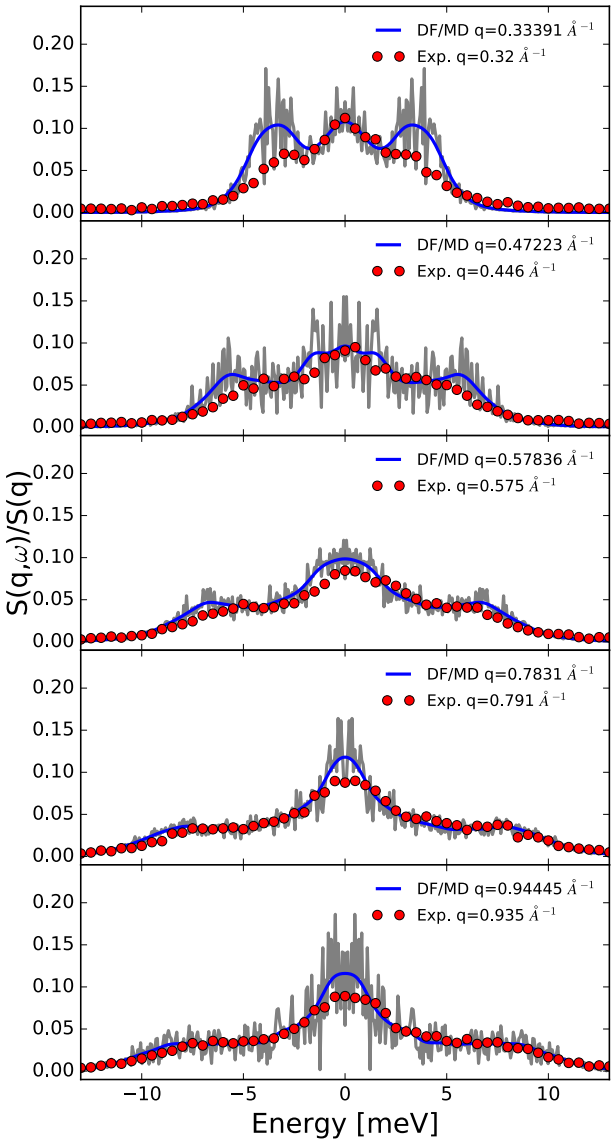

FIG. 3. Ratio of dynamical to static structure factors, $S(q,\omega)/S(q)$, for selected q values at 1023 K. Grey: DF/MD results, blue: DF/MD with 3 meV Gaussian broadening, red: experimental IXS (Ref. 51).

The dispersion relations obtained from the peaks of $C_L(q,\omega)$ are shown in Fig. 6 and can be summarized as follows. There is a linear relationship between ω and q for the low-frequency (<0.6 Å^{-1}) diffusive modes which is followed by a relatively dispersionless range between 0.7 and 1.5 Å^{-1}. Dispersion curves with less pronounced flattening have been found in this region for Cu and Fe,[4] whereas simple liquid metals show a sinusoidal behavior.[1] Particularly striking is the deep minimum near q = 2.0 Å, which is close to the reciprocal lattice vector where a minimum occurs in the phonon spectrum of crystalline Bi.[50] A second, weaker minimum occurs at approximately twice this wave vector. This does not imply that the modes are "phononlike," but it does suggest that a process resembling umklapp scattering can occur in liquids as well as solids. The overall agreement between the calculated dispersion and that derived from IXS data at 573 K[12] is very good, especially in the linear low q range.

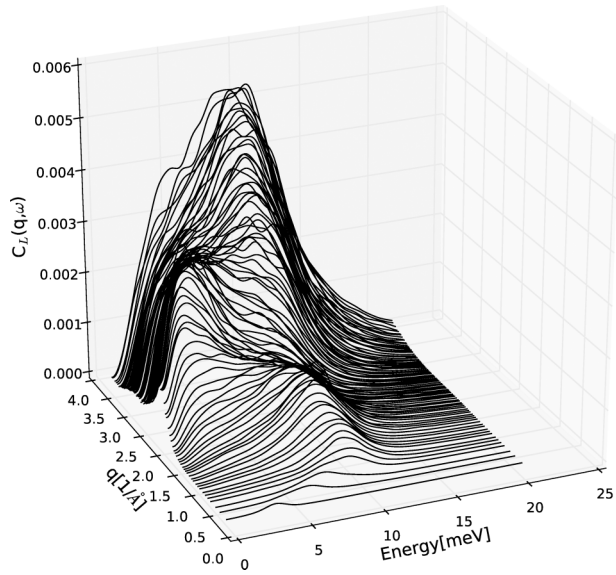

FIG. 4. 3D plot of longitudinal current correlation function, $C_L(q,\omega)$, for 573 K trajectory.

The dispersion at low q values is shown in Fig. 7, and the agreement with experiment is again very good. From the linear part of the dispersion curves, it is possible to calculate the sound velocities, and linear fits to the low q values are shown in Fig. 7 as solid lines. The fit at 573 K gives a sound velocity (LA) of 2070 m/s, compared with the measured adiabatic sound velocity of 1640 m/s at the melting point (544 K).[52,53] The fit at 1023 K yields a sound velocity of 1900 m/s. The analysis of the inelastic neutron scattering data of Sani *et al.*[23] indicated that the low frequency (hydrodynamic) value of the sound velocity (1680 ± 80 m/s) of the LA mode changed to 2005 ± 120 m/s in the range $0.15 \le q \le 0.6$ Å^{-1}, a feature that is referred to as "positive dispersion."

Side peaks of the calculated $C_T(q,\omega)$ spectra provide information about the transverse modes, but they are much weaker than those in $C_L(q,\omega)$. The data have been analyzed here by fitting the quasi-elastic contribution at long wavelength

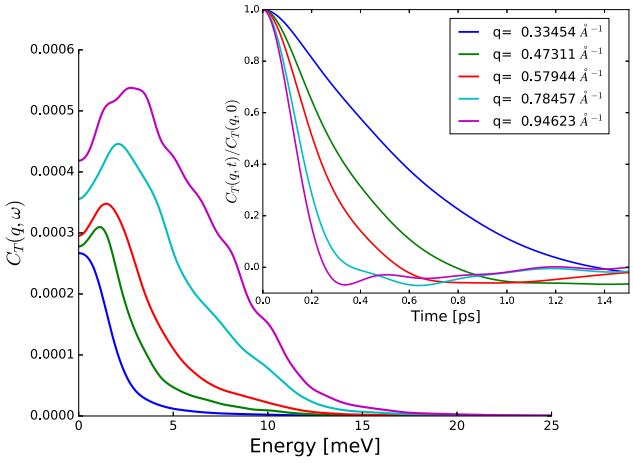

FIG. 5. Calculated transverse current correlation function $C_T(q,\omega)$ and (inset) $C_T(q,t)/C_T(q,0)$ for selected q-values at 573 K.

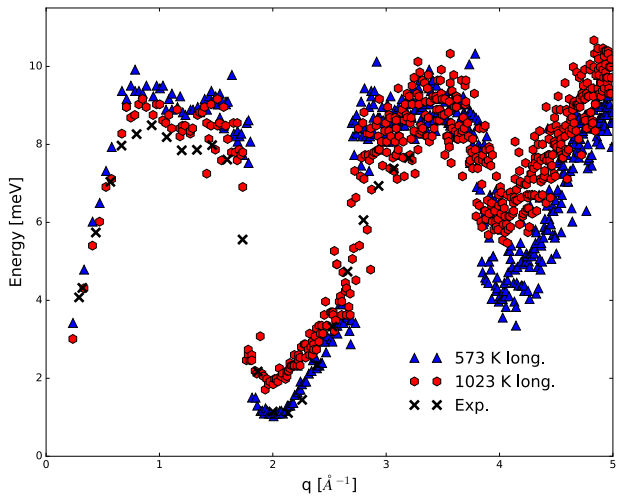

FIG. 6. Longitudinal dispersion of 573 K (blue triangles) and 1023 K (red hexagons) up to q = 5.0 Å^{-1}. Black crosses are experimental results for 573 K of Inui *et al.* (Ref. 12).

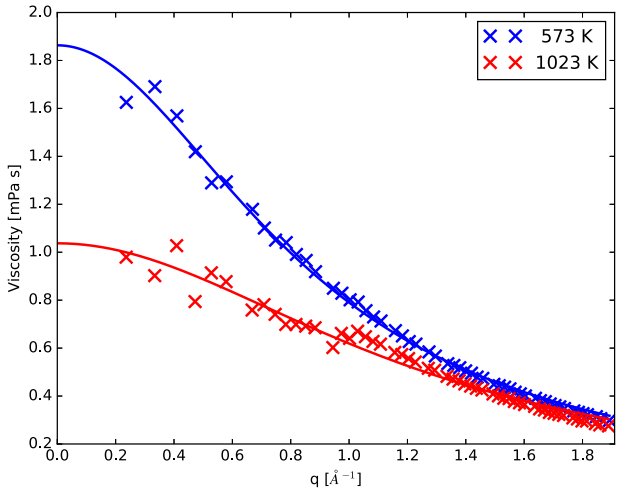

FIG. 8. Viscosity calculated from transverse current correlation function for 573 K (blue) and 1023 K (red). Crosses: calculated values (Eq. (10)), lines: for each q value. Lines are Eq. (11) fitted to values from Eq. (12) to estimate viscosity at $q = 0$.

to a Lorentzian function[39] and determining the peak position by fitting a single Gaussian function to the remainder. The transverse dispersion curves so obtained are also shown in Fig. 7. The dispersion of the TA modes is linear at 573 K (to 1.0 Å^{-1}) and 1023 K (to 0.7 Å^{-1}). The corresponding sound velocities (TA) are 427 m/s for 573 K and 395 m/s for 1023 K. Previous simulations show peaks in $C_T(q,\omega)$ at 600 K for a wide range of q, but no peak at the lowest value of q accessible (0.386 Å^{-1}).[11]

D. Viscosity

The calculation of the q-dependent shear viscosity from the transverse current correlation function [Eq. (11)] is discussed in Sec. II B 4. This function is then extrapolated to the limit $q \to 0$ using Eq. (12), and the results are shown for 573 K and 1023 K in Fig. 8. The calculated shear viscosities are 573 K: 1.86 (1.65) mPa s, 773 K: 1.42 (1.18) mPa s, 923 K: 1.11 (1.06) mPa s, and 1023 K: 1.08 (0.94) mPa s, where the values in brackets are experimental values interpolated from the table of Assael *et al.*[30] The latter were determined by analyzing data of several groups, and there is considerable scatter in the primary data. The most recent data[54] give viscosities that are ~10% higher than the above values. In view of this and of the uncertainties in the extrapolation to q = 0 (Fig. 8), the overall agreement is satisfactory.

The Stokes-Einstein relationship [Eq. (13)] between viscosity η and diffusion constant D was derived for a very simple model, but it is often satisfied fairly well (within ~20%) for monatomic liquids. If we assume that the diameter d of a Bi sphere corresponds to the first peak in the pair distribution function (3.23 Å for all temperatures) and adopt the values of D determined by the TwoPT program (Table I), we find the following values of η using the SER: 573 K: 2.07, 773 K: 1.56, 923 K: 1.27, 1023 K: 1.14 [$10^{-5} \times$ cm^2/s]. These are all approximately 10% higher than the extrapolated values of η given above.

Souto *et al.*[11] also examined the SER in the context of their simulations of Bi at 600 K. Using d = 3.30 Å (the main peak of the pair distribution function) and the calculated value of D, they find a value of η (2.09 mPa s) that is also larger than their value calculated directly from the coordinates and velocities (1.70 ± 0.10 mPa s).

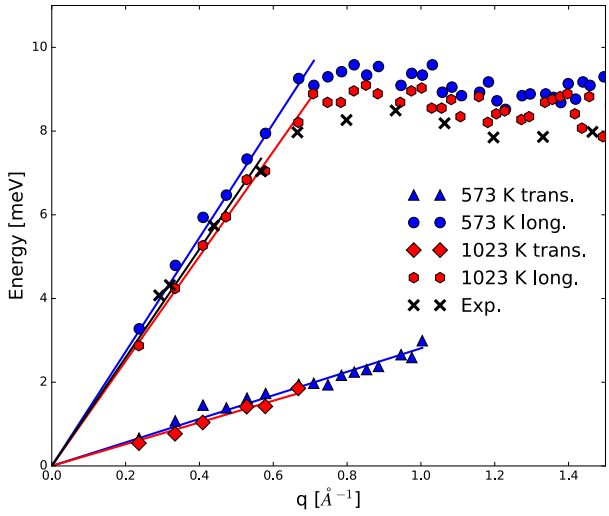

FIG. 7. Longitudinal and transverse dispersion curves for 573 K and 1023 K. Blue circles (triangles) are longitudinal (transverse) modes at 573 K. Red hexagons (diamonds) are longitudinal (transverse) modes at 1023 K. Blue and red lines are the linear fits of the corresponding dispersion modes. Black crosses are experimental results for 573 K (Ref. 12).

IV. DISCUSSION

The results of extensive density functional/molecular dynamics simulations of liquid bismuth (more than 500 atoms, up to 100 ps, four temperatures from 573 K to 1023 K) have been analyzed to provide dynamical information. The use of fitting functions has been minimized to reduce bias on the results. The following conclusions can be drawn:

1. The dynamical structure factor $S(q,\omega)$ agrees well with recent IXS measurements at 573 K[12] and 1023 K,[51] and we emphasize again that no scaling parameters are involved in the comparisons shown in Figs. 2 and 3. Side peaks in $S(q,\omega)$ indicate the presence of collective excitations, and the agreement with the dispersion found in INS,[23] IXS,[12,51] and with other DF/MD calculations[11,12] is very good. $S(q,\omega)$ shows pronounced minima near $q = 2.0$ Å^{-1} and $q = 4.0$ Å^{-1}, close to the minima found in the phonon spectra of Bi crystals.
2. The low-q dispersion shows a sound velocity (2070 m/s, 573 K) that is ∼20% higher than the measured adiabatic sound velocity at the melting point (1640 m/s, 544 K).[52,53] This "positive dispersion" agrees with the measurements and calculations cited above.
3. The spectra of the transverse current correlation functions $C_T(q,\omega)$ show inelastic peaks at 573 K (up to $q \sim 1.0$ Å^{-1}) and 1023 K (to $q \sim 0.7$ Å^{-1}) with linear dispersions corresponding to much lower sound velocities (427 m/s and 395 m/s, respectively) than in the LA modes at low q.
4. The shear viscosity $\eta(q)$ has been calculated from the Laplace transform of the transverse current correlation function $C_T(q,t)$. The extrapolation to $q = 0$ gives values of η at the four temperatures that are ∼10% larger than measured values, which show considerable scatter. The Stokes-Einstein relationship between viscosity η and diffusivity D is satisfied to within ∼10% at all four temperatures.

The agreement between the present calculations, INS and IXS measurements, and other DF calculations will encourage the use of DF/MD simulations in other liquids. The use of simulation cells containing more than 500 atoms has enabled us to obtain improved statistics and extend the range of wave vectors down to 0.23 Å^{-1}. Moreover, the solution of the Kohn-Sham equations means that we avoid the uncertainties associated with approximate kinetic energy functionals commonly used in orbital-free DF calculations.

SUPPLEMENTARY MATERIAL

See supplementary material for comparison of the calculated (DF/MD) and IXS (Refs. 12 and 51) dynamical structure factors $S(q,\omega)$ as a function of ω at 573 K (15 values of q) and 1023 K (15 values of q).

ACKNOWLEDGMENTS

We thank H. R. Schober for valuable discussions and suggestions, M. Inui for supplying original IXS data (Refs. 12 and 51), T. A. Pascal for advice on using the TwoPT program, and S. Kohara for providing starting geometries based on reverse Monte Carlo analysis of XRD data. We acknowledge gratefully the computer time provided by the JARA-HPC Vergabegremium on the JARA-HPC partition of the supercomputer JUQUEEN at Forschungszentrum Jülich and for time granted on the supercomputer JUROPA (Jülich Supercomputer Centre) and at the CSC-IT Center for Science (Espoo, Finland). J.A. and M.R. acknowledge financial support from the Academy of Finland through its Centres of Excellence Program (Project No. 284621).

[1]V. M. Giordano and G. Monaco, Phys. Rev. B **79**, 020201 (2009).
[2]S. Hosokawa, M. Inui, Y. Kajihara, K. Matsuda, T. Ichitsubo, W.-C. Pilgrim, H. Sinn, L. E. González, D. J. González, S. Tsutsui, and A. Q. R. Baron, Phys. Rev. Lett. **102**, 105502 (2009).
[3]S. Hosokawa, S. Munejiri, M. Inui, Y. Kajihara, W.-C. Pilgrim, Y. Ohmasa, S. Tsutsui, A. Q. R. Baron, F. Shimojo, and K. Hoshino, J. Phys.: Condens. Matter **25**, 112101 (2013).
[4]S. Hosokawa, M. Inui, Y. Kajihara, S. Tsutsui, and A. Q. R. Baron, J. Phys.: Condens. Matter **27**, 194104 (2015).
[5]M. Zanatta, F. Sacchetti, E. Guarini, A. Orecchini, A. Paciaroni, L. Sani, and C. Petrillo, Phys. Rev. Lett. **114**, 187801 (2015).
[6]R. O. Jones, Rev. Mod. Phys. **87**, 897 (2015).
[7]A. Delisle, D. J. González, and M. J. Stott, Phys. Rev. B **73**, 064202 (2006).
[8]N. Jakse and A. Pasturel, Phys. Rev. B **79**, 144206 (2009).
[9]L. E. González and D. J. González, Phys. Rev. B **77**, 064202 (2008).
[10]S. Şengül, D. J. González, and L. E. González, J. Phys.: Condens. Matter **21**, 115106 (2009).
[11]J. Souto, M. M. G. Alemany, L. J. Gallego, L. E. González, and D. J. González, Phys. Rev. B **81**, 134201 (2010).
[12]M. Inui, Y. Kajihara, S. Munejiri, S. Hosokawa, A. Chiba, K. Ohara, S. Tsutsui, and A. Q. R. Baron, Phys. Rev. B **92**, 054206 (2015).
[13]S. Munejiri, F. Shimojo, and K. Hoshino, Phys. Rev. B **86**, 104202 (2012).
[14]R. M. Khusnutdinoff and A. V. Mokshin, JETP Lett. **100**, 39 (2014).
[15]N. Jakse and A. Pasturel, Sci. Rep. **3**, 3135 (2013).
[16]F. Hummel, G. Kresse, J. C. Dyre, and U. R. Pedersen, Phys. Rev. B **92**, 174116 (2015).
[17]M. Marqués, L. E. González, and D. J. González, Phys. Rev. B **92**, 134203 (2015).
[18]H. Jones, Proc. R. Soc., London, Sect. A **147**, 396 (1934).
[19]R. E. Peierls, *Quantum Theory of Solids* (Oxford University Press, Oxford, 1955), pp. 108–114.
[20]M. Mayo, E. Yahel, Y. Greenberg, and G. Makov, J. Phys.: Condens. Matter **25**, 505102 (2013).
[21]Y. Greenberg, E. Yahel, E. N. Caspi, C. Benmore, B. Beuneu, M. P. Dariel, and G. Makov, Europhys. Lett. **86**, 36004 (2009).
[22]U. Dahlborg and L. G. Olsson, J. Phys. F: Met. Phys. **13**, 555 (1983).
[23]L. Sani, L. E. Bove, C. Petrillo, and F. Sacchetti, J. Non-Cryst. Solids **353**, 3139 (2007).
[24]K. Shibata, S. Hoshino, and H. Fujishita, J. Phys. Soc. Jpn. **53**, 899 (1984).
[25]J. Akola, N. Atodiresei, J. Kalikka, J. Larrucea, and R. O. Jones, J. Chem. Phys. **141**, 194503 (2014).
[26]CPMD V3.17 © IBM Corp 1990-2013, © MPI für Festkörperforschung Stuttgart, 1997-2001.
[27]N. Troullier and J. L. Martins, Phys. Rev. B **43**, 1993 (1991).
[28]S. G. Louie, S. Froyen, and M. L. Cohen, Phys. Rev. B **26**, 1738 (1982).
[29]J. P. Perdew, A. Ruzsinszky, G. I. Csonka, O. A. Vydrov, G. E. Scuseria, L. A. Constantin, X. Zhou, and K. Burke, Phys. Rev. Lett. **100**, 136406 (2008).
[30]M. J. Assael, A. E. Kalyva, K. D. Antoniadis, R. M. Banish, I. Egry, J. T. Wu, E. Kaschnitz, and W. A. Wakeham, High Temp.-High Pressures **41**, 161 (2012).
[31]J. Kalikka, J. Akola, and R. O. Jones, Phys. Rev. B **90**, 184109 (2014).
[32]T. H. Lee and S. R. Elliott, Phys. Rev. B **84**, 094124 (2011).
[33]S. Kohara, private communication (2014).
[34]S. Nosé, J. Chem. Phys. **81**, 511 (1984); W. G. Hoover, Phys. Rev. A **31**, 1695 (1985).
[35]S.-T. Lin, M. Blanco, and W. A. Goddard, J. Chem. Phys. **119**, 11792 (2003).
[36]M. P. Desjarlais, Phys. Rev. E **88**, 062145 (2013).
[37]P. H. Berens, D. H. J. Mackay, G. M. White, and K. R. Wilson, J. Chem. Phys. **79**, 2375 (1983).
[38]F. J. Harris, Proc. IEEE **66**, 51 (1978).
[39]J.-P. Hansen and I. R. McDonald, *Theory of Simple Liquids*, 4th ed. (Academic Press, Oxford, 2013).
[40]T. Gaskell and S. Miller, J. Phys. C: Solid State Phys. **11**, 4839 (1978).

[41]B. J. Palmer, Phys. Rev. E **49**, 359 (1994).
[42]B. Hess, J. Chem. Phys. **116**, 209 (2002).
[43]U. Balucani, J. P. Brodholt, P. Jedlovszky, and R. Vallauri, Phys. Rev. E **62**, 2971 (2000).
[44]W. E. Alley and B. J. Alder, Phys. Rev. A **27**, 3158 (1983).
[45]A. Einstein, Ann. Phys. (Leipzig) **322**, 549 (1905).
[46]U. Balucani, R. Vallauri, and T. Gaskell, Phys. Rev. A **35**, 4263 (1987).
[47]N. Jakse, J. F. Wax, and A. Pasturel, J. Chem. Phys. **126**, 234508 (2007).
[48]H. R. Schober and H. L. Peng, Phys. Rev. E **93**, 052607 (2016).
[49]N. Jakse and A. Pasturel, J. Chem. Phys. **144**, 244502 (2016).
[50]J. L. Yarnell, J. L. Warren, R. G. Wenzel, and S. H. König, IBM J. Res. Dev. **8**, 234 (1964).
[51]M. Inui, private communication (2016).
[52]O. J. Kleppa, J. Chem. Phys. **18**, 1331 (1950).
[53]S. Blairs, Phys. Chem. Liq. **45**, 399 (2007).
[54]S. Mudry, Y. Plevachuk, V. Sklyarchuk, and A. Yakymovych, J. Non-Cryst. Solids **354**, 4415 (2008).